Bioinspired Fabrication of Hierarchically Structured, pH-Tunable Photonic Crystals with Unique Transition

Qingqing Yang,[†] Shenmin Zhu,[†,*] Wenhong Peng,[†] Chao Yin,[†] Wanlin Wang,[†] Jiajun Gu,[†] Wang Zhang,[†] Jun Ma,[‡] Tao Deng,[†] Chuanliang Feng,[†] and Di Zhang[†,*]

[†]State Key Laboratory of Metal Matrix Composites, Shanghai Jiao Tong University, Shanghai 200240, People's Republic of China, and [‡]School of Engineering, University of South Australia, SA5095, Australia

ABSTRACT We herein report a new class of photonic crystals with hierarchical structures, which are of color tunability over pH. The materials were fabricated through the deposition of polymethylacrylic acid (PMAA) onto a *Morpho* butterfly wing template by using a surface bonding and polymerization route. The amine groups of chitosan in *Morpho* butterfly wings provide reaction sites for the MAA monomer, resulting in hydrogen bonding between the template and MAA. Subsequent polymerization results in PMAA layers coating homogenously on the hierarchical photonic structures of the biotemplate. The pH-induced color change was detected by reflectance spectra as well as optical observation. A distinct U transition with pH was observed, demonstrating PMAA content-dependent properties. The appearance of the unique U transition results from electrostatic interaction between the $-NH_3^+$ of chitosan and the $-COO^-$ groups of PMAA formed, leading to a special blue-shifted point at the pH value of the U transition, and the ionization of the two functional groups in the alkali and acid environment separately, resulting in a red shift. This work sets up a strategy for the design and fabrication of tunable photonic crystals with hierarchical structures, which provides a route for combining functional polymers with biotemplates for wide potential use in many fields.

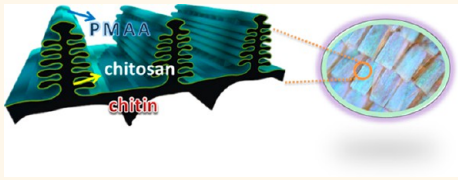

KEYWORDS: biological templates · photonic crystals · polymerization · pH-tunable · functional polymer

Photonic crystals (PCs) with tunability in the visible or near-infrared region are of great significance in controlling light for display, sensor, "smart" medical dressings, or telecommunication device.[1] Functional materials play an essential role in the PC tunability because these materials are able to switch photonic band gaps under external stimuli, such as magnetic field,[2] temperature,[2] mechanical force,[3] or pH.[4] Smart polymers, a major type of functional materials, are perfect candidates for the development of tunable PCs, owing to their volume changes upon external stimuli.[5] A pioneering work by Asher[6] produced a thermally tunable diffracting array based on embedding a crystalline colloidal array of polystyrene spheres within a poly(*N*-isopropylacrylamide) hydrogel. Subsequent work[4,7] found that photonic gels showed volume expansions and contractions in response to changes of pH gradient and accordingly exhibited various structural colors.

Recently, three-dimensional (3D) functional structures have emerged as a topic of growing interest in materials chemistry, especially in the fields of optics, chemical sensing, and microfluidics.[4] Much work focused on the fabrication of 3D pH=responsive PCs by using templating or self-organizing methods, such as polymerized crystalline colloidal arrays,[7] opal hydrogel,[8] or inverse opal hydrogel,[4,8−10] all of which exhibit uniform structures. In fact, PCs with hierarchical structures are believed to demonstrate outstanding performance. Potyrailo reported[11,12] that *Morpho* butterfly wings demonstrated a highly selective reflectance spectrum response to a variety of vapors and liquids of various concentrations, due to their hierarchical photonic crystal structures with interconnected micropores and special capillary condensation. Recently, modification has been attempted to intensify the natural hierarchical structure through padding nanotubes into the space of the butterfly scales, producing a unique infrared sensor.[13] Therefore, smart polymers engineered with hierarchical photonic structures are expected to present high performance. Unfortunately,

* Address correspondence to smzhu@sjtu.edu.cn, zhangdi@sjtu.edu.cn.

Received for review January 9, 2013 and accepted May 19, 2013.

Published online May 20, 2013
10.1021/nn400090j

© 2013 American Chemical Society

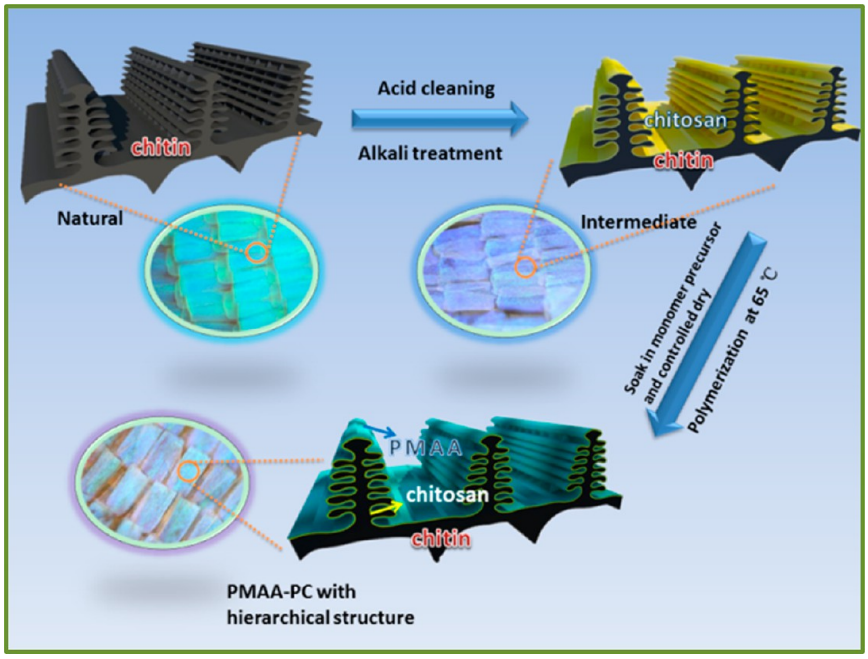

Scheme 1. Overall synthesis of pH-responsive PCs from Morpho butterfly wings: (1) the butterfly wings pretreated with HCl were carefully dipped into a 10 wt % NaOH solution to transform the wing surface chitin into chitosan; (2) this modified template was immersed into MAA precursors and then brought out removing excess surface liquid; and (3) the polymerization occurred on the template surface, resulting in PMAA PCs of hierarchical structures (PMAA-PC).

hierarchical photonic structures with the combination of complex macro-, meso-, and even nanoscales are still a challenge to model.[14]

Our previous studies have reported a direct biotemplate method for synthesizing various functional ceramic replicas from natural periodic structures, including TiO_2, ZnO, ZrO_2, and SnO_2.[15−18] Very recently, a sol−gel route followed by reduction has been developed for the preparation of magnetophotonic crystal Fe_3O_4 from *Morpho* butterfly wings (MPC-Fe_3O_4), and the resultant MPC-Fe_3O_4 demonstrated a novel optical and magnetic coupling effect.[19] Nevertheless, these approaches are not suitable for the fabrication of polymer−photonic crystals with hierarchical structures for two reasons below. First, the formation of pores and tiny structural details is a great challenge for polymers; that is, the pores tend to be closed or fractured by plastic deformation of the walls during fabrication. Second, the nanostructure formation is entropically limited for polymers, that is, the entropic restriction of conformations in the nanoconfinement of particles and thin walls.[9,20,21] In this article, for the first time, we report a new class of photonic crystals of hierarchical structures by using a surface bonding and polymerization route. The PCs are fabricated by tailoring a coating of polymethylacrylic acid (PMAA) on the surface of *Morpho* butterfly wings (PMAA-PC). Our PCs demonstrate a significant U-shaped pH response.

RESULTS AND DISCUSSION

Scheme 1 illustrates the overall process of pH-responsive PC synthesis from *Morpho* butterfly wings. First, *Morpho* butterfly wings were surface-treated by alkali to transform the surface chitin into chitosan, and then PMAA was deposited on the wing surface by *in situ* polymerization, resulting in PMAA photonic crystals of hierarchical structures (PMAA-PC). For the PMAA-PC-1, -2, and -3, the content of PMAA deposited on the samples increases gradually with its monomer concentration in the precursor.

We first investigated the structure of a *Morpho* butterfly wing. Its front side shows a shining blue color (Figure 1a) that derives from arrays of vertically aligned net-like skeleton structures[22] (Figure 1b). A typical dimension of a scale is at ∼200 μm in length and ∼75 μm in width. These overlapping scales possess an overall rectangular shape as demonstrated in Figure 1b. Thirty five to 40 rows of ridges are found to align themselves on the scale surface with an almost identical interspacing. Figure 1c reveals the porous architecture of this scale. Each scale comprises parallel ridges, which are spaced several micrometers apart and aligned along the scale longitudinal direction. These ridges supported by cross-ribs hold the lamellae 500 nm over the scale bottom surface. A cross section view of these lamellae is shown in Figure 1d. The ∼2 μm high ridges are decorated by 6−7 lamellas, each of which is around 450 nm wide and 100 nm thick; these ridges are spaced approximately 700 nm apart, and the upper ridges and ribs are supported by columnar pillars which are located on a bottom layer in Figure 1d.[11] The color is caused by vertical branch-like structures made from alternating layers of air and cuticles.

SEM was employed to characterize and compare the morphologies of the intermediate alkali-treated template

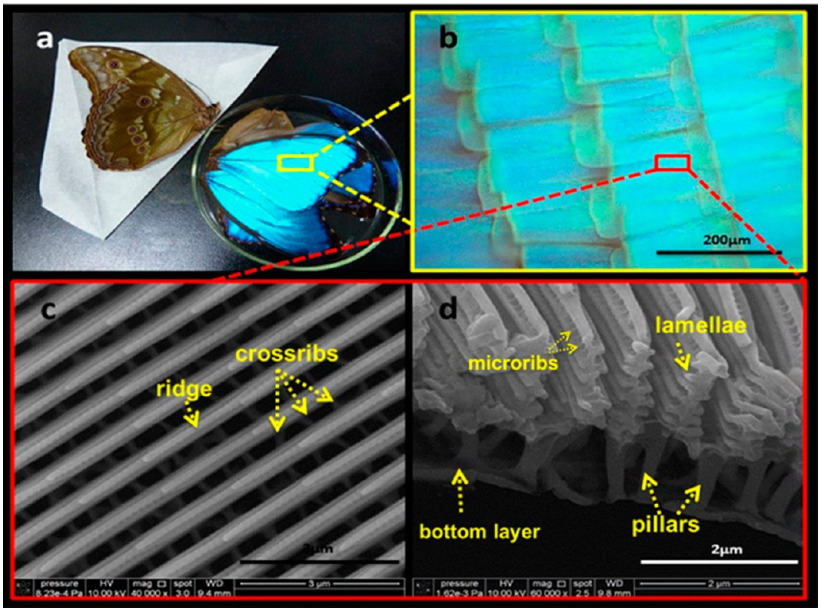

Figure 1. Characterization of natural Morpho butterfly wings: (a) digital image of intact butterfly, (b) optical microscopy image of the wing scales from the wing front, and SEM images of the ground blue scale (c) from a vertical view and (d) from a horizontal view.

and PMAA-PCs (Figure 2 and Supporting Information Figure S1). At low magnification, both PMAA-PCs (Figure S1b–d) and the alkali-treated template (Figure S1a) consist of scales that have parallel ridges. The fine nanoscale ribs, inherited from alkali-treated butterfly wings, are well preserved in PMAA-PCs, as evidenced by the high-magnification micrograph (Figure 2b–d). The smooth surface of all PMAA-PC samples indicates the homogeneous polymerization of PMAA on butterfly wings. Designed with the highest monomer concentration, PMAA-PC-3 exhibits the most obvious layers of PMAA coated on the surface as compared with PMAA-PC-1 and PMAA-PC-2. In brief, PMAA-PCs inherited the intricate and highly interconnected network of the original wing scales through our fabrication.

The PMAA content in PMAA-PCs was determined by TGA analysis. When temperature reaches 600 °C, the biotemplate residue is at ~9 wt % (Figure S2a) while neat PMAA is completely exhausted (Figure S2a). The larger percentage of PMAA in PMAA-PC, the less percentage of residues at 600 °C. According to the TGA result, the residues of PMAA-PC-1, -2, and -3 were at around 24, 16, and almost 0, respectively. Thus, PMAA-PC-3 has the highest PMAA content, followed by PMAA-PC-2 and PMAA-PC-1.

Further investigation of PMAA content in PMAA-PCs was carried out by X-ray photoelectron spectroscopy (XPS). Typical peaks for C1s, N1s, and O1s are observed for both *Morpho* butterfly wings and PMAA-PCs (Figure S3). Two peaks at 288 and 285 eV indicate a considerable degree of carbon oxidation. The binding energy values of 284.67, 285.9, and 287.1 eV are caused by the non-oxygenated ring C (C–H), C in C–O or C–N, and C in C═O, respectively. With the deposition of PMAA on the butterfly surface, a new binding energy appears at 289 eV, corresponding to carboxyl C (COOH, 289.1 eV) (Figure S3b–d,f–h). On the basis of the relative intensity of these peaks, the C–N ratios of PMAA-PC-1, PMAA-PC-2, and PMAA-PC-3 were calculated to be 10.82, 11.18, and 15.73, respectively (Supporting Information, Table S1).[23] Both TGA and XPS evidence proved that PMAA was combined with the biotemplate and that the weight content of PMAA increased gradually from PMAA-PC-1 to PMAA-PC-2 to PMAA-PC-3.

Fourier transform infrared (FTIR) spectroscopy was conducted to investigate whether there is an interaction between chitosan and PMAA. Regarding the original butterfly wings (Figure S4a), the characteristic absorption lines of amide groups are at 1651 cm^{-1} (–C═O, amide I vibration), 1548 cm^{-1} (–NH_2 bonding in non-acetylated 2-aminoglucose primary amine, amide II vibration), and 1378 cm^{-1}(–N–H stretching or C–N bond stretching vibrations, amide III vibration). The absorption lines at 1157, 1115, 1075, and 1029 cm^{-1} might be the vibrational motion of characteristic C–O bonds. Compared with the original wings, the amide in the wings was obviously stronger after the alkali treatment (Figure S4b). This is due to the transformation of the chitin of butterfly wings into chitosan that provides the –NH_2 functional groups for bonding with the –COOH of the monomer MAA. A new absorption line at 1714 cm^{-1} is observed in the final PMAA-PCs (Figure S4c), contributing to vibration of the carboxyl group in PMAA, in comparison with an absorption line at 1720 cm^{-1} for neat PMAA (Figure S4d). Compared with the biotemplate, the absorption line of the N–H bond at 1549.8 cm^{-1} shifts to 1538.7 cm^{-1} and the O–H vibration is split from 3285.9 to 3289.5 cm^{-1}, due to the hydrogen bonding between carboxyl groups of PMAA and amino or hydroxyl groups of chitosan.[24]

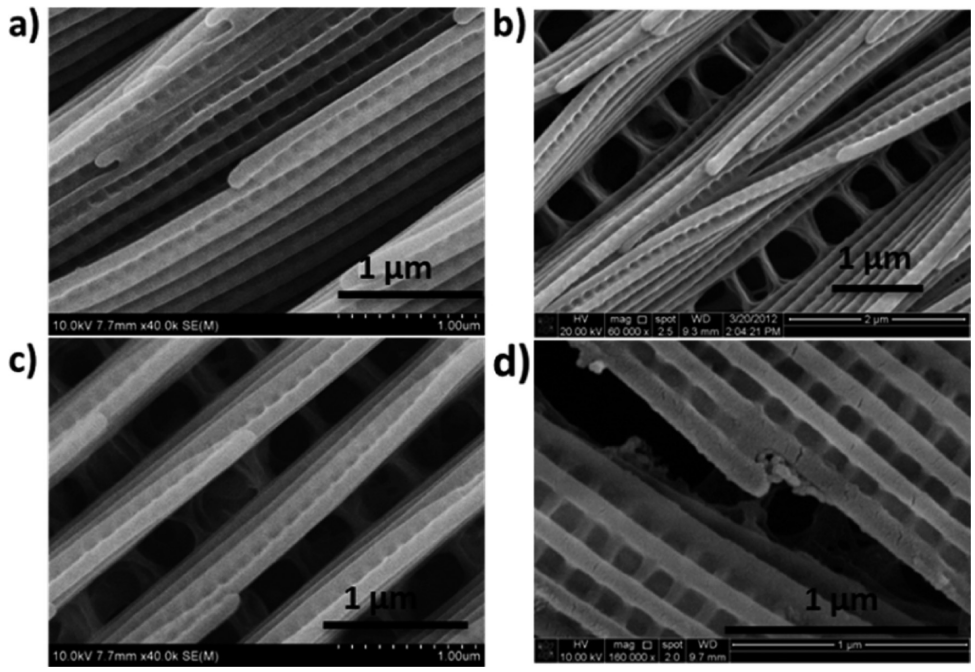

Figure 2. SEM micrographs of (a) alkali-treated template, (b) PMAA-PC-1, (c) PMAA-PC-2, and (d) PMAA-PC-3.

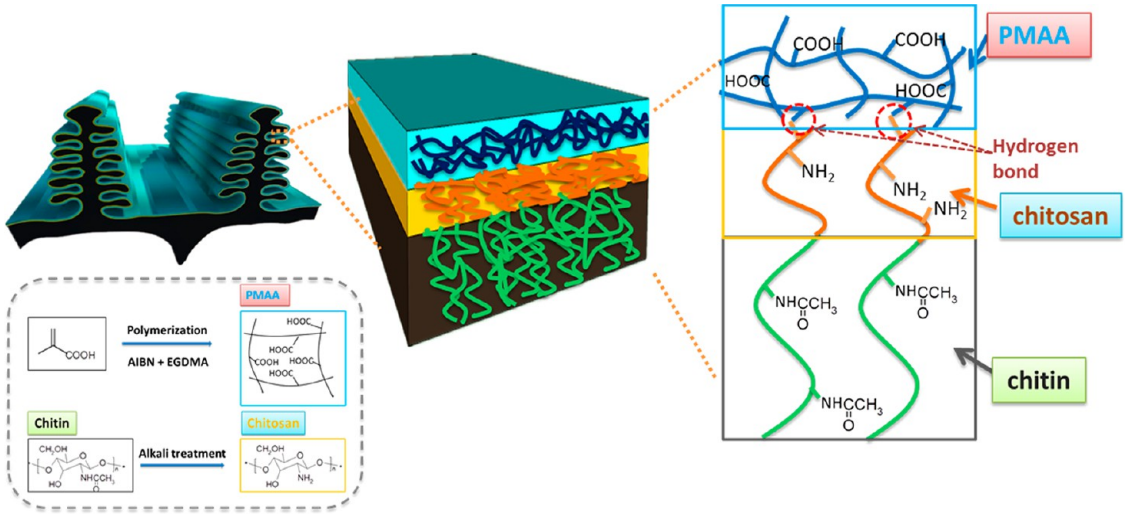

Scheme 2. Schematic illustration of the formation mechanism for pH-tunable photonic crystals with hierarchical structures (PMAA-PC).

On the basis of the foregoing discussion, it is reasonable to conclude that PMAA with fine hierarchical photonic structures obtained from the biotemplate can be prepared by this impregnation and polymerization method. In this process, the hydrogen bonding between the two functional groups −COOH of PMAA and $-NH_2$ of the biotemplate must have a crucial effect on the uniform coating. To prove the importance of the reaction, PNIPA (poly(*N*-isopropylacrylamide)) was deposited on the surface of *Morpho* butterfly wings using a similar process (Figure S5, Supporting Information); the PNIPA dispersion on the biotemplate is not uniform at all because there is no reaction between PNIPA and the biotemplate. We propose a synthesis mechanism in Scheme 2. The alkali treatment of butterfly wings provides reactive groups ($-NH_2$) on the wing surface, which can react with the −COOH of monomers to form hydrogen bonding. The monomers then polymerize to produce long chains homogeneously coating on the wing scales to produce a smooth surface, corresponding to our SEM and XPS analysis. As a result, this pH-responsive PMAA was introduced into the photonic crystals of hierarchical structures.

PMAA-PCs were investigated by using a spectrophotometer. The original butterfly wing exhibits the strongest reflection at around 467 nm (spectrum a in Figure 3a), which is a bright blue color (Scheme 1) owing to its unique photonic crystal structure.[25] The

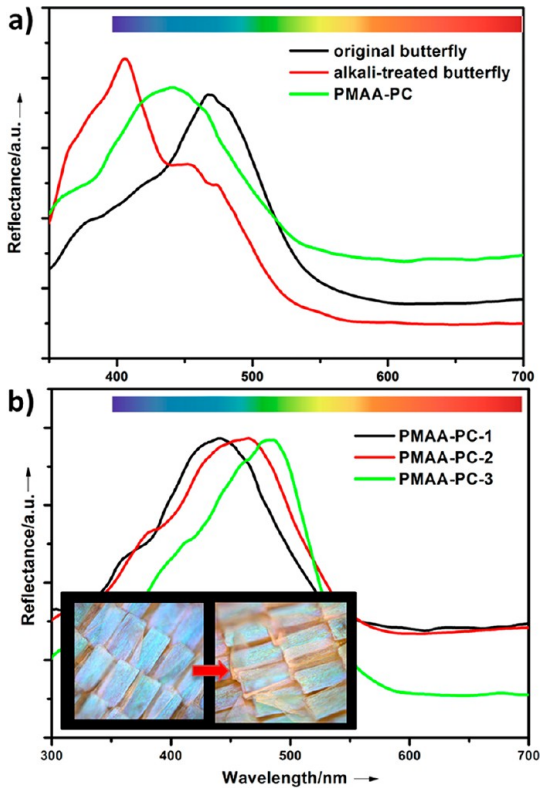

Figure 3. (a) Reflection spectra of original butterfly wing, the alkali-treated butterfly wings, and the final PMAA-PC samples. (b) PMAA-PC-1, PMAA-PC-2, and PMAA-PC-3. The insets are the optical images of PMAA-PC-1 and PMAA-PC-3.

biotemplate shows a blue-shift reflection peak at 405 nm (spectrum b in Figure 3a), while the final PC demonstrates a red-shift reflection peak at 438 nm. These are ascribed to two reasons: (i) the difference in refractive indexes (RI) of chitin (RI = 1.56),[26] chitosan (RI = 1.59),[27] and PMAA (RI = 1.41);[28] and (ii) the slight variation of periodical scale.

With the increase in PMAA content from PMAA-PC-1 to PMAA-PC-2 to PMAA-PC-3, the highest reflective peak exhibits an obvious red shift (Figure 3b). In particular, PMAA-PC-1 is light blue (λ_{max} = 438 nm) and PMAA-PC-3 appears green-blue (λ_{max} = 483 nm) (Figure 3b insets).

The spectral properties were evaluated through varying the external pH stimuli (Figure 4−6). Figure 4 shows how λ_{max} varies with the biotemplate pH. The diffraction resonance shifts from 465.5 to 491.5 nm when pH decreases from 10.51 to 1.62, consistent with the color change from blue to green. This red shift is attributed to the protonation of $-NH_2$ groups under low pH values, inducing a volume expansion due to ionic repulsion.[29]

The λ_{max} dependences on pH for PMAA-PC-1, PMAA-PC-2, and PMAA-PC-3 are demonstrated in Figure 5. In comparison with the biotemplate (Figure 4), all three PMAA-PCs display a distinct transition at certain pH values, with each PMAA-PC demonstrating similar maximum reflection except the U point. Figure S6

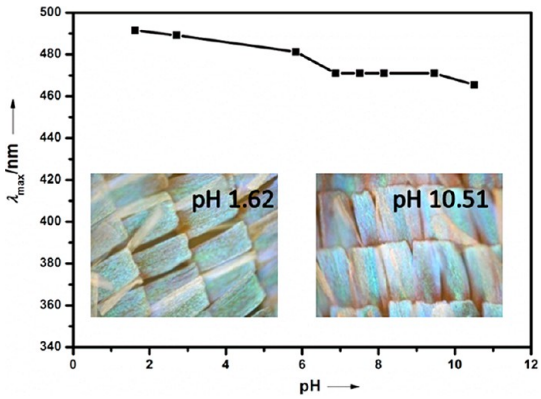

Figure 4. Dependence of diffraction resonance on pH for the biotemplate and its corresponding representative optical images (insets).

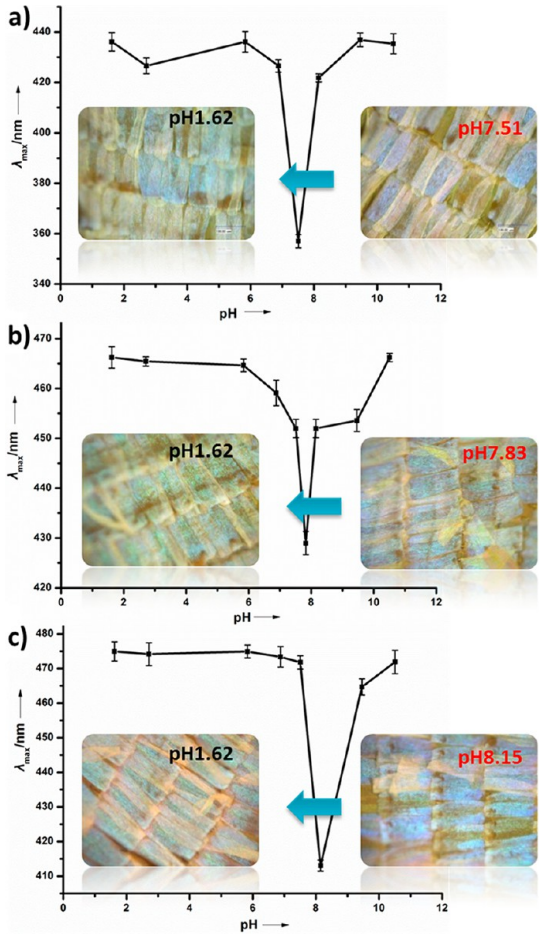

Figure 5. Representative spectral responses of (a) PMAA-PC-1, (b) PMAA-PC-2, and (c) PMAA-PC-3 to different pH values, with representative optical images obtained at typical pH values.

shows the spectra of PMAA-PC-1, -2, and -3 near and in the U point. Specifically, U transitions for PMAA-PC-1, PMAA-PC-2, and PMAA-PC-3 occur at around pH 7.51, 7.83, and 8.15, respectively. It is the content of PMAA covered on the template that induced a shift of the U transition pH value from 7.51 to 8.15. Correspondingly,

the optical image of each PMAA-PC agrees with its reflection spectrum.

For instance, the color of PMAA-PC-1 (Figure 5a) is blue at pH 1.62, where the highest reflection peak is at ~436 nm; the reflective blue color was observed with increases in pH until 7.51, where it turns to violet with a λ_{max} of 357 nm. With a further pH increase to 10.51, the reflection reverts to its original wavelength (around 438 nm) and the color changes back to blue. A similar trend was seen for PMAA-PC-2 and PMAA-PC-3 (Figure 5b,c), but all of these samples demonstrate different initial spectrum peak positions that correspond to different initial colors. In brief, these materials are pH-responsive with unique U transitions.

In order to further investigate the durability of the PMAA-PCs, we tested the spectrum response of the sample in a changed pH evironment for a few cycles. Figure 6 shows the reversible change in λ_{max} of PMAA-PC-1 as pH varies. It can be seen that the PMAA-PC-1 swells and deswells reversibly, indicating a satisfied durability of the PMAA-PC.

On the basis of the foregoing discussion, we propose a mechanism for the optical properties of PMAA-PCs. For the alkali-treated wing scales, when the pH decreases gradually, the $-NH_2$ groups of chitosan (the chitosan pK_a 6.2–6.8[30]) are protonated and transformed to $-NH_3^+$ groups, which causes swelling because of electrostatic self-repulsion. Thus, the reflectance spectrum exhibits a red-shift phenomenon due to the changed refractive index,[4] as evidenced in Figure 5; *vice versa*, chitosan deswelling is caused by the deprotonation of the $-NH_2$ as the pH increases beyond the chitosan pK_a. By contrast, the swelling/deswelling behavior of pure PMAA is opposite. With an increase in pH, a large amount of carboxyl groups inside the PMAA (the PMMA pK_a ~5.5[31]) are deprotonated, and the charged $-COO^-$ groups repel each other and lead to the swelling behavior. Lowering pH induces the PMMA deswelling due to the decrease in PMAA ionization.[32] In conclusion, the volume change determines the periodical structures of samples and thus their optical properties.

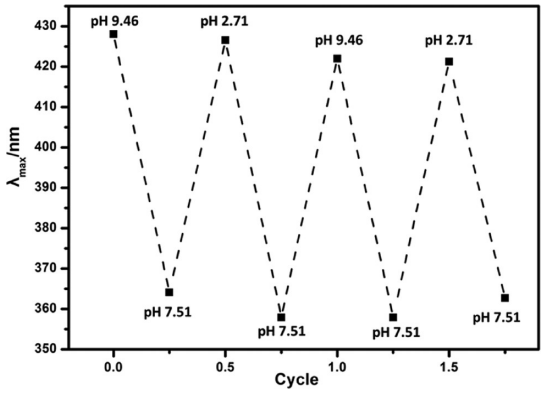

Figure 6. Evaluating the reversibility of the diffraction resonance at multiple cyclings of the pH value.

It has been reported that simulation can help to clarify the mechanism and to predict the structure and properties of the designed product. In 2012, Lee used a numerical simulation to predict the reflection point of inverse opal pH sensors based on protic monomers copolymerized with polyhydroxyethylmethacrylate hydrogel. The discrepancy reflection point by ~1 pH scale was found between the experimental result and simulation, which is explained by the charge repulsion effect between the bond anions of polymers.[32] Our system is totally different. First, there are two kinds of responsive polymer—PMAA and chitosan. Second, there exists an interaction between PMAA and chitosan. Finally, the retained rigid biotemplate of chitin will influence the response. Therefore, Lee's model cannot be used in our system. Even so, on the basis of the experimental results, the unique U-shaped responsive property can be explained by the contrary protonation and deprotonation behaviors of both $-NH_2$ and $-COOH$ groups in PMAA-PC (Scheme 3).

Taking PMAA-PC-1 as an example, the U transition point is at pH 7.51, where the whole volume is the most compacted, as evidenced by the blue-shifted reflectance peak. At this point, strong electrostatic interaction occurs

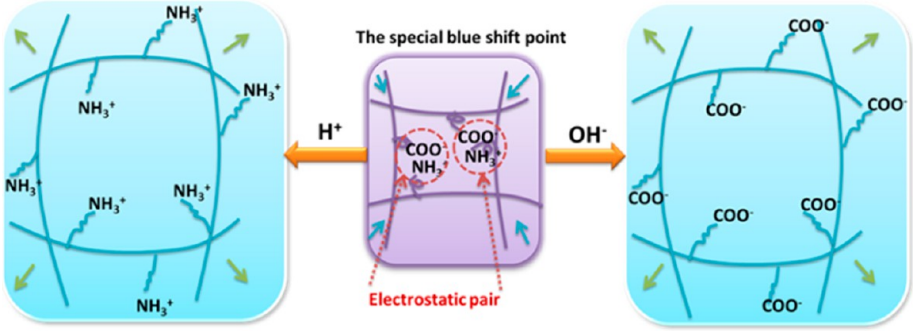

Scheme 3. Mechanism for the U-shaped pH response of PMAA-PC. At a special blue-shift point, strong electrostatic interaction occurs between $-COO^-$ groups in PMAA and $-NH_3^+$ groups in chitosan, leading to the deswelling of the whole specimen.[33] At acidic pH, the sample swells due to two possible reasons: first, the protonation of a carboxylate ion in $-COO^-NH_3^+$ breaks up its electronic pairs; second, more positive charges are introduced by the protonation of primary amino group, which additionally favors the expansion of the system. In contrast, with pH increasing to an alkali environment, the dissociation of the electrostatic $-COO^-NH_3^+$ ionic pairs introduced by deprotonation of the $-NH_3^+$ group and the deprotonation of carboxyl leads to the expanding of the system.

between $-COO^-$ groups in PMAA and $-NH_3^+$ groups in chitosan, which leads to the deswelling of the whole specimen.[33] At acidic pH, the sample swells due to two possible reasons: first, the protonation of carboxylate ionic in $-COO^-NH_3^+$ breaks up its electronic pairs; and second, more positive charges are introduced by the protonation of primary amino group, which additionally favors the expansion of the system. With pH increasing to an alkali environment (above pH 7.51), the swelling phenomenon also can be explained by two reasons: first, the deprotonation of the $-NH_3^+$ group results in the dissociation of the electrostatic $-COO^-NH_3^+$ ionic pairs; second, the deprotonation of carboxyl produces many negative charges, expanding the system. That is why the U transition occurs within a very narrow pH range. To the best of our knowledge, most of the previously reported pH-responsive PCs show either red shift or blue shift with the variation of pH.[34] Our PMMA-PCs, cost-effectively fabricated by a biomimetic method, is the first time demonstration of a unique tailorable U-shaped pH response.

CONCLUSION

In summary, a novel surface bonding and polymerization route was developed to fabricate pH-tunable photonic crystals of hierarchical structures, combining natural photonic crystals with a pH-responsive polymer (PMAA-PCs). PMAA-PCs exhibits a unique U-shaped pH response, due to (i) the electrostatic interaction between $-NH_3^+$ of chitosan and the $-COO^-$ groups of PMAA formed, leading to a special blue-shifted point at the pH value of U transition; and (ii) the ionization of the two functional groups in the alkali and acid environment separately, resulting in a red shift. Interestingly, the U point, where the whole system shows the largest shrinkage, demonstrates a PMAA content-dependent functionality. Since these unique U-shaped amphiprotic-responsive photonic crystals are capable of converting chemical energy into characteristic optical signals, our biomimetic technique would provide an effective approach to the synthesis of stimuli-responsive materials of hierarchical photonic structures, which have a great potential for label-free chemicals, biological detections, pH analysis, and photonic switches. Although the butterfly scales are small and fragile, our research result offers a novel idea and valuable data support for the artificial analogies of 3D functional PCs, such as nanoimprinting[35] and focused-ion-beam chemical-evaporation-deposition (FIB-CVD)[36] methods which are non-template-involved. Besides, our method, applying a layer of PMAA homogeneously on the hierarchical photonic crystal structure of the biotemplate, provides a route for combining functional polymers with biotemplates for potential use in many fields.

METHODS

Materials. The *Morpho* butterfly wings we chose as biotemplates were supplied by Shanghai Natural Wild-Insect Kingdom Co., Ltd. Methylacrylic acid (MAA), H_3PO_4, $NaH_2PO_4 \cdot 2H_2O$, $Na_2HPO_4 \cdot 12H_2O$, NaCl, HCl, NaOH, Na_2CO_3, and $NaHCO_3$ were purchased from Sinopharm Chemical Reagent Co., Ltd. Ethylene glycol dimethylacrylate (EGDMA) was obtained from Aladdin Chemistry Co., Ltd. 2,2′-Azobis(isobutyronitrile) (AIBN) was supplied by the Shanghai No.4 Reagent & HvChemical Co., Ltd. MAA and AIBN were distilled before use to remove polymerization inhibitor.

Preparation of PMAA-PCs. Scheme 1 illustrates the overall process of the pH-responsive PC synthesis from *Morpho* butterfly wings. It contains the following steps: (1) the butterfly wings, pretreated with 6 wt % HCl, were carefully dipped into a 10 wt % NaOH solution at 60 °C for 15 min to transform the surface chitin of the original butterfly into chitosan; (2) the modified template was immersed into MAA monomer precursors at room temperature for 24 h, and then brought out, removing excess surface liquid with filter paper through a capillary; and (3) the polymerization occurred on the surface of the biotemplate when the temperature increased from room temperature to 65 °C for 24 h, resulting in pH-responsive photonic crystals with hierarchical structures (PMAA-PC). The precursor is actually a mixture of 4 mL of MAA monomer (47.16 mmol), 2 mL of cross-linking agent EGDMA (10.59 mmol), 0.01 g of AIBN (6.1 mmol) as an initiator, and some anhydrous ethanol as solvent. To modulate the PMAA content in the product, the concentration of MAA monomer in the precursor increased from 40.9 to 52.6 to 65.1 wt %, producing PMAA-PC-1, PMAA-PC-2, and PMAA-PC-3, respectively.

Characterization of the Samples. Scanning electron microscopy was performed on a JEOL JSM-6360LV field emission microscope at an accelerating voltage of 15 kV. Fourier transform infrared measurements (FT-IR) were recorded on KBr pellets with a PE Paragon 1000 spectrophotometer. X-ray photoelectron spectra (XPS) were collected on a physical electronics PHI5400 using Mg K radiation as the X-ray source. All of the spectra were corrected with the C1s (285.0 eV) band. Thermal gravimetric analysis (TGA) was conducted on a PE TGA-7 instrument at 10 °C · min^{-1}. A 20/20 PV UV−visible−NIR micro-spectrophotometer was used to study the optical properties. The digital optical photographs of these samples were taken using a KEYENCE three-dimensional stereo-microscope.

Characterization of pH-Responsive Properties. In order to investigate the pH-responsive optical property, each sample was immersed into buffer solution for about 5 min to reach equilibrium and then mounted into a cuvette of a UV−vis spectrometer. At normal incidence, optical readings about reflectance were sequentially recorded as the pH was gradually varied from 10.51 to 1.62. Note that the local ionic strength also has an effect on the response. Here, we only focused on the pH dependence with a constant ionic strength.[37]

Conflict of Interest: The authors declare no competing financial interest.

Acknowledgment. The authors gratefully acknowledge the financial support of the Morgan Crucible Company, the National Science Foundation of China (Nos. 51171110, 51072117), National Basic Research Program of China (973 Program, 2012CB619600, 2011CB922200, 20120073130001), Shanghai Science and Technology Committee (0JC1407600). We also thank the Shanghai Jiao Tong University (SJTU) Instrument Analysis Center.

Supporting Information Available: Additional characterization details of SEM images, thermal gravimetric analyses, XPS spectra, FTIR and reflectance spectra. This material is available free of charge *via* the Internet at http://pubs.acs.org.

REFERENCES AND NOTES

1. Holtz, J. H.; Asher, S. A. Polymerized Colloidal Crystal Hydrogel Films as Intelligent Chemical Sensing Materials. *Nature* **1997**, *389*, 829–832.

2. Xu, X.; Friedman, G.; Humfeld, K. D.; Majetich, S. A.; Asher, S. A. Superparamagnetic Photonic Crystals. *Adv. Mater.* **2001**, *13*, 1681–1684.
3. Foulger, S. H.; Jiang, P.; Lattam, A. C.; Smith, D.; Ballato, J. Mechanochromic Response of Poly(ethylene glycol) Methacrylate Hydrogel Encapsulated Crystalline Colloidal Arrays. *Langmuir* **2001**, *17*, 6023–6026.
4. Lee, Y. J.; Braun, P. V. Tunable Inverse Opal Hydrogel pH Sensors. *Adv. Mater.* **2003**, *15*, 563–566.
5. Shibayama, M.; Tanaka, T. Volume Phase Transition and Related Phenomena of Polymer Gels. *Adv. Polym. Sci.* **1993**, *109*, 1–62.
6. Weissman, J. M.; Sunkara, H. B.; Tse, A. S.; Asher, S. A. Thermally Switchable Periodicities and Diffraction from Mesoscopically Ordered Materials. *Science* **1996**, *274*, 959–960.
7. Lee, K.; Asher, S. A. Photonic Crystal Chemical Sensors: pH and Ionic Strength. *J. Am. Chem. Soc.* **2000**, *122*, 9534–9537.
8. Aguirre, C. I.; Reguera, E.; Stein, A. Tunable Colors in Opals and Inverse Opal Photonic Crystals. *Adv. Funct. Mater.* **2010**, *20*, 2565–2578.
9. Wang, J.; Cao, Y.; Feng, Y.; Yin, F.; Gao, J. Multiresponsive Inverse-Opal Hydrogels. *Adv. Mater.* **2007**, *19*, 3865–3871.
10. Shin, J.; Braun, P. V.; Lee, W. Fast Response Photonic Crystal pH Sensor Based on Templated Photo-Polymerized Hydrogel Inverse Opal. *Sens. Actuators, B* **2010**, *150*, 183–190.
11. Potyrailo, R. A.; Ghiradella, H.; Vertiatchikh, A.; Dovidenko, K.; Cournoyer, J. R.; Olson, E. *Morpho* Butterfly Wing Scales Demonstrate Highly Selective Vapour Response. *Nat. Photonics* **2007**, *1*, 123–128.
12. Yang, X.; Peng, Z.; Zuo, H.; Shi, T.; Liao, G. Using Hierarchy Architecture of *Morpho* Butterfly Scales for Chemical Sensing: Experiment and Modeling. *Sens. Actuators, A* **2011**, *167*, 367–373.
13. Pris, A. D.; Utturkar, Y.; Surman, C.; Morris, W. G.; Vert, A.; Zalyubovskiy, S.; Deng, T.; Ghiradella, H. T.; Potyrailo, R. A. Towards High-Speed Imaging of Infrared Photons with Bio-Inspired Nanoarchitectures. *Nat. Photonics* **2012**, *6*, 195–200.
14. Li, F.; Josephson, D. P.; Stein, A. Colloidal Assembly: The Road from Particles to Colloidal Molecules and Crystals. *Angew. Chem., Int. Ed.* **2011**, *50*, 360–388.
15. Chen, Y.; Zang, X.; Gu, J.; Zhu, S.; Su, H.; Zhang, D.; Hu, X.; Liu, Q.; Zhang, W.; Liu, D. ZnO Single Butterfly Wing Scales: Synthesis and Spatial Optical Anisotropy. *J. Mater. Chem.* **2011**, *21*, 6140–6143.
16. Chen, Y.; Gu, J.; Zhu, S.; Fan, T.; Zhang, D.; Guo, Q. Iridescent Large-Area ZrO_2 Photonic Crystals Using Butterfly as Templates. *Appl. Phys. Lett.* **2009**, *94*, 053901–053903.
17. Zhu, S.; Zhang, D.; Chen, Z.; Gu, J.; Li, W.; Jiang, H.; Zhou, G. A Simple and Effective Approach towards Biomimetic Replication of Photonic Structures from Butterfly Wings. *Nanotechnology* **2009**, *20*, 3153031–3153038.
18. Liu, X.; Zhu, S.; Zhang, D.; Chen, Z. Replication of Butterfly Wing in TiO_2 with Ordered Mesopores Assembled Inside for Light Harvesting. *Mater. Lett.* **2010**, *64*, 2745–2747.
19. Peng, W.; Zhu, S.; Wang, W.; Zhang, W.; Gu, J.; Hu, X.; Zhang, D.; Chen, Z. 3D Network Magnetophotonic Crystals Fabricated on *Morpho* Butterfly Wing Templates. *Adv. Funct. Mater.* **2012**, *22*, 2072–2080.
20. Jiang, P.; Hwang, K.; Mittleman, D.; Bertone, J.; Colvin, V. Template-Directed Preparation of Macroporous Polymers with Oriented and Crystalline Arrays of Voids. *J. Am. Chem. Soc.* **1999**, *121*, 11630–11637.
21. Johnson, S. A.; Ollivier, P. J.; Mallouk, T. E. Ordered Mesoporous Polymers of Tunable Pore Size from Colloidal Silica Templates. *Science* **1999**, *283*, 963–965.
22. Yoshioka, S.; Kinoshita, S. Wavelength-Selective and Anisotropic Light-Diffusing Scale on the Wing of the *Morpho* Butterfly. *Proc. R. Soc. London, Ser. B* **2004**, *271*, 581–587.
23. Xing, Y.; Sun, X.; Li, B. Poly(methacrylic acid)-Modified Chitosan for Enhancement Adsorption of Water-Soluble Cationic Dyes. *Polym. Eng. Sci.* **2009**, *49*, 272–280.
24. Ahn, J. S.; Choi, H. K.; Cho, C. S. A Novel Mucoadhesive Polymer Prepared by Template Polymerization of Acrylic Acid in the Presence of Chitosan. *Biomaterials* **2001**, *22*, 923–928.
25. Kinoshita, S.; Yoshioka, S. Structural Colors in Nature: The Role of Regularity and Irregularity in the Structure. *ChemPhysChem* **2005**, *6*, 1442–1459.
26. Vigneron, J. P.; Rassart, M.; Vandenbem, C.; Lousse, V.; Deparis, O.; Biró, L. P.; Dedouaire, D.; Cornet, A.; Defrance, P. Spectral Filtering of Visible Light by the Cuticle of Metallic Woodboring Beetles and Microfabrication of a Matching Bioinspired Material. *Phys. Rev. E* **2006**, *73*, 0419051–0419058.
27. Domard, A.; Rinaudo, M. Preparation and Characterization of Fully Deacetylated Chitosan. *Int. J. Biol. Macromol.* **1983**, *5*, 49–52.
28. Pristinski, D.; Kozlovskaya, V.; Sukhishvili, S. A. Determination of Film Thickness and Refractive Index in One Measurement of Phase-Modulated Ellipsometry. *J. Opt. Soc. Am. A* **2006**, *23*, 2639–2644.
29. Aime, S.; Crich, S. G.; Botta, M.; Giovenzana, G.; Palmisano, G.; Sisti, M. A Macromolecular Gd(III) Complex as pH-Responsive Relaxometric Probe for MRI Applications. *Chem. Commun.* **1999**, *16*, 1577–1578.
30. Schmuhl, R.; Krieg, H.; Keizer, K. Adsorption of Cu(II) and Cr(VI) Ions by Chitosan: Kinetics and Equilibrium Studies. *Water SA* **2004**, *27*, 1–8.
31. Topham, P. D.; Howse, J. R.; Crook, C. J.; Gleeson, A. J.; Bras, W.; Armes, S. P.; Jones, R. A. L.; Ryan, A. J. Autonomous Volume Transitions of a Polybase Triblock Copolymer Gel in a Chemically Driven pH-Oscillator. *Macromol. Symp.* **2007**, *256*, 95–104.
32. Shin, J.; Han, S. G.; Lee, W. Inverse Opal pH Sensors with Various Protic Monomers Copolymerized with polyHEMA Hydrogel. *Anal. Chim. Acta* **2012**, *752*, 87–93.
33. Kozlovskaya, V.; Sukhishvili, S. A. Amphoteric Hydrogel Capsules: Multiple Encapsulation and Release Routes. *Macromolecules* **2006**, *39*, 6191–6199.
34. Wang, J.; Han, Y. Tunable Multiresponsive Methacrylic Acid Based Inverse Opal Hydrogels Prepared by Controlling the Synthesis Conditions. *Langmuir* **2009**, *25*, 1855–1864.
35. Saito, A.; Miyamura, Y.; Ishikawa, Y.; Murase, J.; Akai-Kasaya, M.; Kuwahara, Y. Reproduction, Mass Production, and Control of the *Morpho* Butterfly's Blue. *Proc. SPIE* **2009**, *7205*, 7205061–7205069.
36. Watanabe, K.; Hoshino, T.; Kanda, K.; Haruyama, Y.; Matsui, S. Brilliant Blue Observation from a *Morpho*-Butterfly-Scale Quasi-structure. *Jpn. J. Appl. Phys.* **2005**, *44*, L48–L50.
37. Piret, F.; Su, B. L. Effects of pH and Ionic Strength on the Self-Assembly of Silica Colloids to Opaline Photonic Structures. *Chem. Phys. Lett.* **2008**, *457*, 376–380.